



# Activation energies of high-volume fly ash ternary blends: Hydration and setting



Dale P. Bentz\*

Engineering Laboratory, National Institute of Standards and Technology, 100 Bureau Drive, Stop 8615, Gaithersburg, MD 20899-8615, United States

## ARTICLE INFO

### Article history:

Received 9 November 2013  
Received in revised form 30 May 2014  
Accepted 20 June 2014  
Available online 17 July 2014

### Keywords:

Apparent activation energy  
Calcium carbonate powder  
High-volume fly ash  
Hydration  
Isothermal calorimetry  
Setting

## ABSTRACT

Because ready-mixed concrete is placed under a wide variety of environmental conditions, the influence of temperature on the hydration reactions and the accompanying setting process is of critical importance. While contractors are generally quite comfortable with the temperature sensitivity of conventional ordinary Portland cement (OPC) concretes, more sustainable mixtures containing high volumes of fly ash (HVFA), for example, often present problems with delayed setting times and increased temperature sensitivity. Based on isothermal calorimetry and Vicat needle penetration measurements, this study demonstrates that the high temperature sensitivity of such HVFA mixtures can be effectively moderated by the replacement of a portion of the fly ash with a fine calcium carbonate powder. In addition to accelerating and amplifying hydration and reducing setting times at a given temperature, the presence of the fine  $\text{CaCO}_3$  powder also lowers the apparent activation energy for setting for temperatures below 25 °C. The reactivity of the  $\text{CaCO}_3$  in these mixtures is quantified using thermogravimetric analysis. Comparison of results for  $\text{CaCO}_3$  powders of nominal sizes of 1  $\mu\text{m}$  and 17  $\mu\text{m}$ , replacing 10% by volume of the cement in an OPC mixture, indicates that the former is highly superior in accelerating/amplifying hydration and reducing setting times.

Published by Elsevier Ltd.

## 1. Introduction

While high volume fly ash (HVFA) concretes have been investigated for many years [1], recent interest in sustainability has created renewed interest in these mixtures. The generally acceptable performance of these mixtures at later ages from both a strength and durability viewpoint is often offset by their reduced constructability, as exemplified by delayed setting times, low early-age strengths, and increased sensitivity to temperature (curing) [2,3]. Recent studies have focused on the ability of calcium carbonate ( $\text{CaCO}_3$ ) powder additions to mitigate the first two of these deficiencies in HVFA concrete mixtures [4–10], with finer (1  $\mu\text{m}$  particle size)  $\text{CaCO}_3$  being particularly efficient in this regard [7–10]. The fine  $\text{CaCO}_3$  particles provide a greatly increased surface area for the precipitation and growth of hydration products [8] and also participate to a small extent in reactions with the cement phases to produce more voluminous [6] and potentially stiffer [11] carboaluminate hydration products. While a few studies have included temperature as a variable [12,13], the former even including an analysis of activation energies for initial and final setting,

neither of them used a  $\text{CaCO}_3$  powder that is as fine as that employed in the present study. In the study of Ezziane et al. [12], for example, the replacement of cement with 5–25%  $\text{CaCO}_3$  on a mass basis resulted in increased setting times under all investigated curing conditions (20 °C, 40 °C, and 60 °C).

Activation energy analysis has been often applied to both hydration and setting processes in cement-based materials [12,14–17], and is, of course, the basis for the well-known and standardized maturity method for predicting in situ concrete strength development [18,19]. The basic premise in an Arrhenius-based approach is that the rate parameter,  $k$ , for the process of interest (hydration, setting, or strength development) is a function of temperature that can be described as:

$$k = Ae^{\left(-\frac{E_A}{RT}\right)} \quad (1)$$

where  $A$  is a kinetics constant,  $E_A$  is the apparent activation energy (typically reported in units of kJ/mol),  $R$  is the universal gas constant [8.314 J/(mol K)], and  $T$  is absolute temperature in K. This equation can be conveniently applied to transform temporally varying results measured at one temperature to a second temperature, a so-called time–temperature transformation. The equivalent time,  $t_e$ , at a reference temperature,  $T_r$ , can be determined as:

\* Tel.: +1 (301)975 5865; fax: +1 (301)990 6891.

E-mail address: [dale.bentz@nist.gov](mailto:dale.bentz@nist.gov)

$$t_e = e \left[ -\frac{E_A}{R} \left( \frac{1}{T_i} - \frac{1}{T_r} \right) \right] \quad (2)$$

where  $T_i$  and  $t$  are the measurement temperature and time, respectively. For example, curing a concrete specimen for 12 h at 40 °C would be equivalent to curing for 26 h at 25 °C, for a system with an apparent activation energy of 40 kJ/mol.

In a similar manner, results obtained at two different temperatures can be analyzed to estimate the apparent activation energy for the process. For two sets of experimental conditions, Eq. (2) can be rearranged to solve for the apparent activation energy as:

$$E_A = \frac{-\ln \left( \frac{t_1}{t_2} \right) R}{\left( \frac{1}{T_2} - \frac{1}{T_1} \right)} \quad (3)$$

Eq. (3) can be applied numerically to specific events, such as the measured initial setting times at two different temperatures in this study, or can be applied graphically to continuous data, such as isothermal calorimetry curves in this study, to assess the value of the apparent activation energy that provides the best overlap of the multiple (transformed) data sets. For example, initial setting times of 2.39 h and 3.93 h measured at 25 °C (298.15 K) and 15 °C (288.15 K), respectively, would correspond to an activation energy of 35.5 kJ/mol according to Eq. (3). The term apparent activation energy is employed to indicate that cement hydration consists of a complex set of reactions, each with its own individual activation energy. Thus, only an apparent value is obtained when analyzing such a system in a simple composite manner. This study investigates the apparent activation energies for hydration and initial setting in a variety of HVFA ternary blends for temperatures of 15 °C, 25 °C, and 40 °C.

## 2. Materials and experimental procedures

Materials employed in this study were equivalent to those utilized in a recent study on sustainable concretes employing high volumes of fly ash and fine (1 μm) CaCO<sub>3</sub> powder [9,10]. A new batch of the Type I/II cement used in the previous study was obtained from a local supplier. According to its mill test certificate report, the cement has a Blaine fineness of 372 m<sup>2</sup>/kg and an estimated Bogue phase composition of 58.5% C<sub>3</sub>S, 11.2% C<sub>2</sub>S, 6.4% C<sub>3</sub>A, and 9.6% C<sub>4</sub>AF on a mass basis, after adjusting for the 3.7% CaCO<sub>3</sub> content of the ground cement powder. The measured oxide compositions and densities of the cement and the two fly ashes used in this study are provided in Table 1. The measured particle size distributions (PSD, laser diffraction with isopropanol as the solvent) of all powder materials are provided in Fig. 1. Both a Class C and a Class F fly ash were examined, with their respective CaO percentages of 24.6% and 0.7% by mass providing a reasonable representation of the expected extremes in these values for the fly ashes commonly available in the US. The Class C fly ash is

**Table 1**  
Oxide composition percent by mass, loss on ignition, and density of the cement and the Class C and Class F fly ashes.

Property	Type I/II cement	Class C fly ash	Class F fly ash
SiO <sub>2</sub> (%)	19.4	38.4	59.7
Al <sub>2</sub> O <sub>3</sub> (%)	4.5	18.7	30.2
Fe <sub>2</sub> O <sub>3</sub> (%)	3.2	5.1	2.8
CaO (%)	62.3	24.6	0.7
MgO (%)	3.4	5.1	0.8
SO <sub>3</sub> (%)	2.9	1.4	0.02
Na <sub>2</sub> O (%)	0.52 eq.	1.7	0.2
K <sub>2</sub> O (%)	See Na <sub>2</sub> O	0.6	2.4
Loss on ignition (%)	2.7	0.3	0.8
Density	3150 ± 10 kg/m <sup>3</sup>	2630 kg/m <sup>3</sup>	2160 kg/m <sup>3</sup>

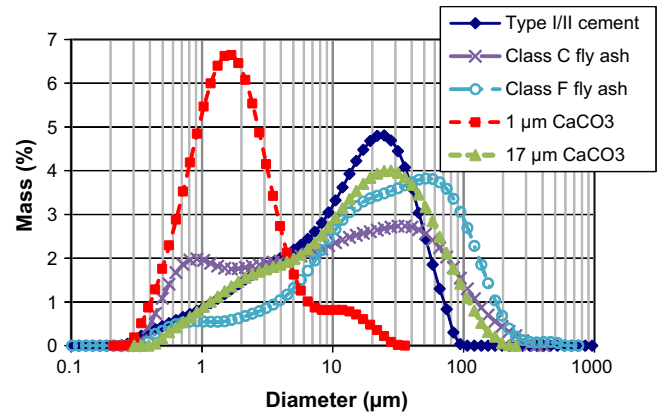


**Fig. 1.** Measured differential particle size distributions for the various powders employed in the present study. Results shown are the average of six individual measurements and error bars (one standard deviation) would fall within the size of the symbols on the plot.

hydraulic and retards cement hydration considerably [7–10]. CaCO<sub>3</sub> powder of two different particle sizes (nominally 1 μm and 17 μm) was used to replace a portion of the cement or fly ash in some mixtures. It has a reported density of 2710 kg/m<sup>3</sup> and a reported MgCO<sub>3</sub> content of 1% by mass. The finer material has a measured (BET) surface area of 9.93 m<sup>2</sup>/g, while the coarser material has a value of 0.83 m<sup>2</sup>/g [8]. No chemical admixtures were employed in the present study of pastes.

To provide the fairest comparison of results, all paste mixtures were prepared utilizing volumetric proportioning, maintaining a constant volume fraction of water and powders (cement, fly ash, and CaCO<sub>3</sub>) [7–10,20], based on a control cement-only paste with a water-to-cement ratio by mass (w/c) of 0.35. Most previous studies, including those in [12,13], have performed mass-based replacements and maintained a constant water-to-solids ratio on a mass basis, thereby confounding the change in water volume fraction (initial porosity) due to the differing densities of cement, fly ash, and CaCO<sub>3</sub> powder with the change in binder chemical composition. Mixtures were prepared where 10% of the cement was replaced by an equal volume of CaCO<sub>3</sub> powder or where either 40% or 60% of the cement by volume was replaced with fly ash–CaCO<sub>3</sub> blends. Mixture designations are summarized in Table 2; for example, C45L15 indicates a paste mixture where 60% of the cement by volume has been replaced, 45% by Class C fly ash and 15% by fine CaCO<sub>3</sub> powder. The performance of the fine and coarse CaCO<sub>3</sub> powders was only contrasted in the Portland cement–CaCO<sub>3</sub> binary blends, as an equivalent contrast in HVFA ternary blends had been conducted previously [8].

All powders for a given mixture were pre-blended for 30 min in a shaker-mixer that employs rotation, translation, and inversion to

**Table 2**  
Powder mixture proportions (volume) and designations.

Designation	% Cement	% F ash	% C ash	% Fine CaCO <sub>3</sub>	% Coarse CaCO <sub>3</sub>
Control	100				
L10	90			10	
L10coarse	90				10
F40	60	40			
F30L10	60	30		10	
C40	60		40		
C30L10	60		30	10	
F60	40	60			
F45L15	40	45		15	
C60	40		60		
C45L15	40		45	15	

homogeneously mix powders of different specific gravities and particle sizes. A total of 33 mixtures were prepared at three different temperatures. To perform analysis of activation energies for both low and elevated temperatures, prepared pastes were targeted for temperatures of 15 °C, 25 °C, or 40 °C at the end of a high shear mixing cycle by pre-cooling the raw materials and mixing at a lower-than-target temperature in an environmental chamber. For the pastes (Table 2) prepared at the three conditions, final average mixture temperatures (with standard deviations) of 15.2 °C ± 1.0 °C, 25.6 °C ± 0.7 °C, and 37.9 °C ± 1.1 °C were achieved. All calorimetry and setting measurements were subsequently conducted under nominally isothermal conditions, the former in an isothermal calorimeter and the latter in a temperature-controlled (±1 °C) climatic chamber. It should be noted that the volume of the frustum specimen employed for setting time measurements is certainly sufficient to generate adequate heat to raise the specimen temperature for a period of time, even in a temperature-controlled chamber. However, this is considered to be of minimal concern in the present study where the focus is on initial setting times, due to the fact that the cumulative heat released through the dormant period and up to the time of initial setting during the acceleratory phase is relatively small.

Isothermal calorimetry was conducted on small paste specimens (≈5 g) in a sealed glass vial, with data acquisition typically being initiated some 30 min after the initial contact of cement and water. This means that the initial heat peak due to the dissolution of cement upon contact with water was not captured in the present experiments. Setting times were assessed using an automated Vicat apparatus, following the ASTM C191 standard procedures [21]. As per the standard, the initial setting time was estimated as the time when a penetration of 25 mm into the paste frustum specimen was achieved. Needle penetration results to follow are presented in terms of penetration resistance, obtained by subtracting the measured penetration from the nominal frustum specimen height of 40 mm (a penetration resistance of 15 mm will therefore correspond to initial setting).

Two small sealed plastic vials of cement paste (≈10 g) from each mixture were prepared and stored at the target temperature for thermogravimetric analysis (TGA) at the ages of 1 d and 7 d. Each of the five initial powders was also analyzed via TGA to estimate their respective calcium hydroxide and calcium carbonate contents. For a TGA scan, the system was first equilibrated at 30 °C and then the temperature was raised to 1000 °C at a rate of 10 °C/min, while flushing with ultra-high purity (UHP) nitrogen at a flow rate of 50 mL/min. Calcium hydroxide content was estimated based on the measured mass loss between 400 °C and 550 °C, while calcium carbonate content was estimated based on the subsequent mass loss between 600 °C and 800 °C. Both of these determinations were conducted on a per g ignited material (final mass at 1000 °C) basis. The raw materials were analyzed using approximately 50 mg of powder, while the hydrated specimens nominally consisted of 100 mg of broken paste fragments. Other than storing the fresh paste specimens in sealed vials and conducting the TGA experiments in UHP nitrogen, no other measures were taken to attempt to minimize their atmospheric carbonation.

### 3. Results and discussion

To provide further support for relevance of the present study in pastes to real world concretes, for nine of the mixtures prepared at 25 °C, their measured initial setting times were contrasted against those previously obtained for mortar (ASTM C403 [22]) sieved from similar concrete mixtures [9,10]. While the control concrete in that study was prepared with a nominal w/c of 0.4 (vs. the 0.35 for the control paste in the present study) and those mixtures

employed various dosages of a high-range water reducer, as can be seen in Fig. 2, the comparison of setting times is generally favorable. This suggests that changes in setting times measured in this paste-only study should indeed carry over to the performance of similar field concrete mixtures.

A representative subset of the needle penetration results are given in Fig. 3, while complete results for isothermal calorimetry are provided in Fig. 4. The heat flow results in Fig. 4 are normalized per mL of water in the mixture, as such a normalization has been found to provide a better correlation with measured compressive strengths [23,24]. The measured apparent activation energies (via Eq. (3)) for setting and hydration based on the 15 °C and 25 °C data sets are listed in Table 3, while those for the 25 °C and 40 °C data sets are given in Table 4. Because the calorimetry results represent heat flow per unit time, to properly transform them from one temperature to another, not only must the time scale on the x-axis be adjusted by an appropriate time–temperature scaling factor, but also the heat flow values on the y-axis must be divided by this same factor. While the same graphical analysis was conducted on the cumulative heat release curves from the calorimetry measurements, presenting the heat flow curves here is more informative for assessing the applicability of a single apparent activation energy in describing the changes in hydration with temperature. Since the setting process is controlled by hydration of the silicate phases (particularly the more reactive tricalcium silicate) in most cases [25,26], the time transformations of the calorimetry data for each mixture were performed to achieve a good match between the onset and initial rise of the primary silicate hydration peaks at each two temperatures being analyzed. The extent of the overlap of the time-transformed curves for each two temperatures provides an indication of the capability of a single apparent activation energy to capture the influence of temperature on cement hydration. In cases where the overlap does not extend beyond the initial silicate hydration peak, the determined apparent activation energy then only accurately represents that portion of the initial (silicate) hydration process.

For needle penetration measurements, the generally good overlap of the time-transformed results in Fig. 3 indicates that, for the temperature range investigated in this study, the setting process at any two temperatures can be described by a single apparent activation energy. However, as can be seen in Tables 3 and 4, the apparent activation energies are significantly different when lowering the temperature vs. when raising it from the nominal room temperature value of 25 °C. The influences of fly ash and fine CaCO<sub>3</sub> on these apparent activation energies will be considered in detail

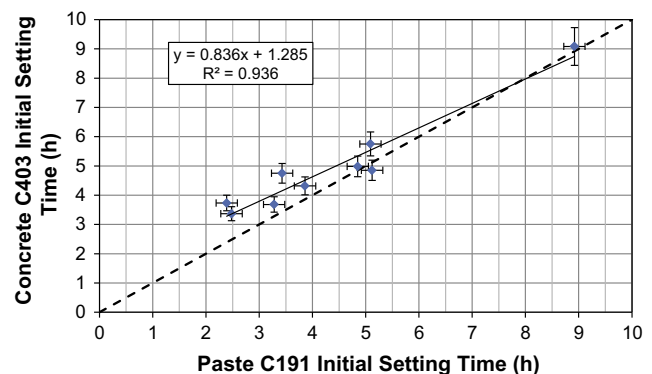


Fig. 2. Comparison of 25 °C paste initial setting times measured in this study to those measured on sieved mortars from 'equivalent' concretes in a previous study [9,10]. The solid line indicates the best-fit linear relationship, while the dashed line indicates a 1:1 relationship. Error bars indicate the single-operator measurement uncertainty according to the relevant ASTM standards [21,22].

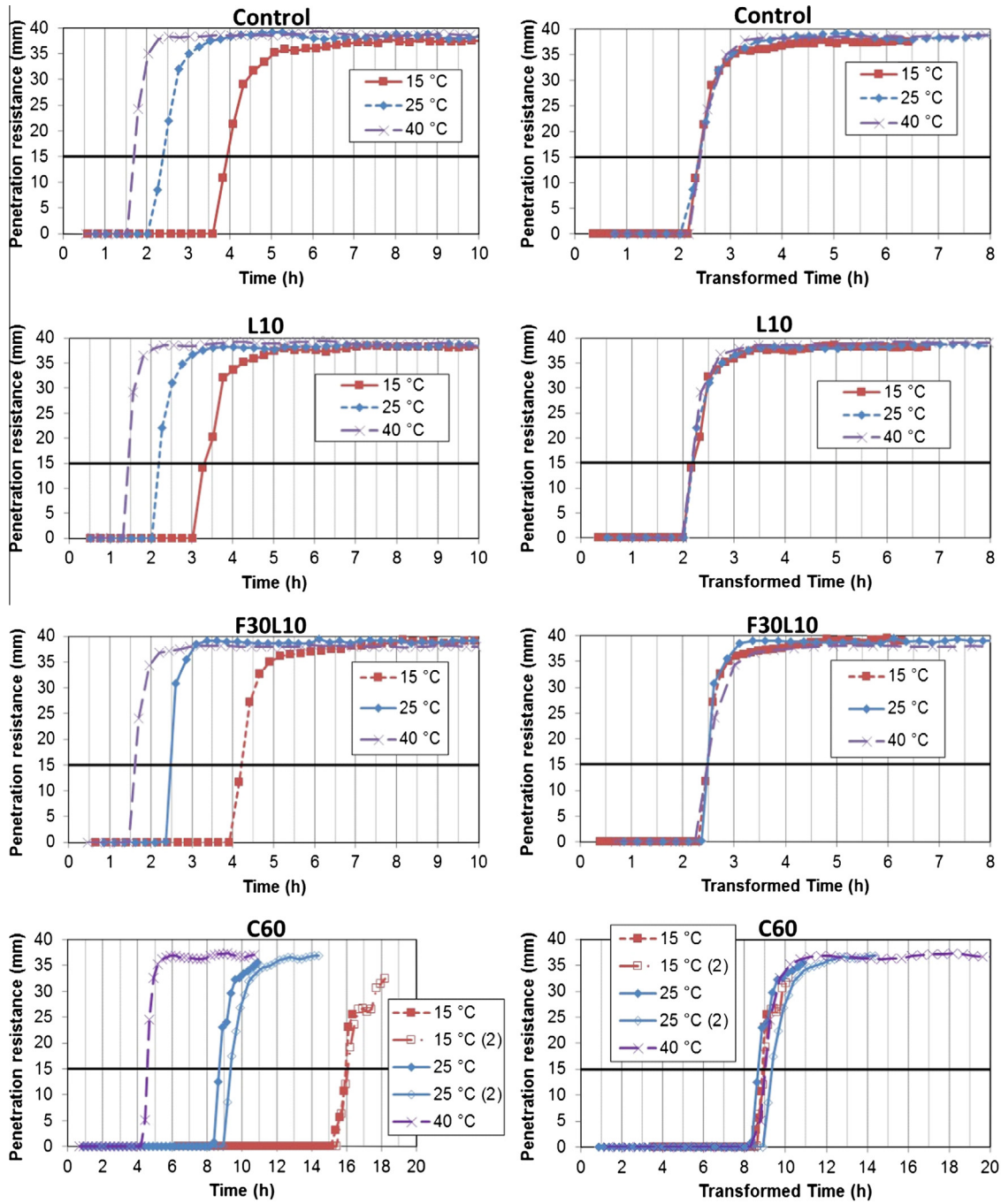
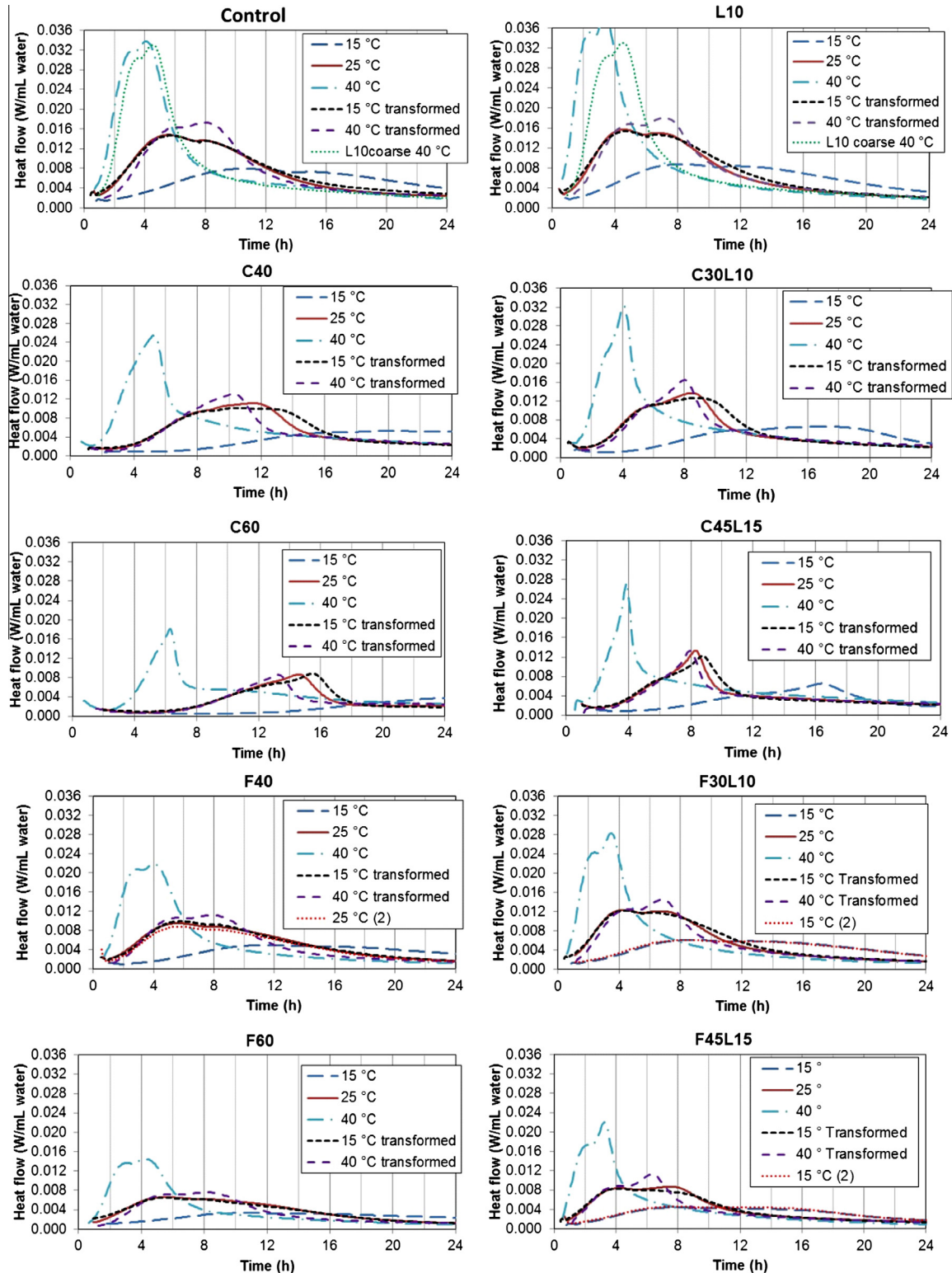


Fig. 3. Comparison of setting measured at different temperatures. Plotted vs. measured time (left) and transformed time (right) for control, L10, F30L10, and C60 systems. Two measurements (separate mixtures) at 15 °C and 25 °C are shown for the C60 system to provide an indication of measurement variability.

subsequently, after first discussing the isothermal calorimetry results for the different mixtures as a function of temperature.

The majority of the heat flow vs. time curves in Fig. 4 exhibit a pattern typical of cements, with a dormant period followed by two overlapping peaks. The first peak is generally attributed to reaction of the silicate phases, while the second one is due to renewed reaction of the aluminate phases, as sulfates are depleted from the pore solution [25]. For the cement, cement with fine CaCO<sub>3</sub> replacement, and mixtures with the Class F fly ash (with or without fine CaCO<sub>3</sub>), one can observe that the transformed 15 °C results basically overlap the original 25 °C data set throughout the first 24 h, suggesting that it is indeed appropriate to use a single apparent activation energy to describe the temperature sensitivity of the

early-age hydration reactions for this limited temperature range. However, for the Class C fly ash mixtures, where the two peaks have merged into a single (somewhat misshapen) peak, matching the initial rises measured at the two temperatures results in the remainder of the 15 °C peak being shifted to longer times relative to the 25 °C curve. This would indicate that the apparent activation energy for the reactions occurring during this phase of the hydration is higher than that determined by only fitting the first part of the calorimetry peak. Note that based on the values in Table 1 (along with the fact that it is hydraulic in its own right), the Class C fly ash has sufficient oxides of calcium, aluminum, and sulfur to participate in the cement's aluminate hydration reactions, which could contribute to the change in apparent activation energy that



**Fig. 4.** Heat flow vs. time plots for the control, 10% fine  $\text{CaCO}_3$  replacement for cement, and eight fly ash– $\text{CaCO}_3$  blends at three temperatures. Transformed data have been obtained based on applying a single time–temperature transformation factor for each temperature pair (15/25 and 25/40). Two measurements (separate mixtures) at 25 °C for the F40 system and 15 °C for the F30L10 and F45L15 systems are shown to provide some indication of measurement variability.

was not observed in the other three (control,  $\text{CaCO}_3$ , Class F fly ash) systems. Conversely, while  $\text{CaCO}_3$  does participate in the aluminate reactions, leading to the formation of carboaluminate as opposed to sulfoaluminate phases [6], it apparently does not significantly change the temperature sensitivity of the reactions. The Class F fly ash, on the other hand, appears to be basically inert during

the first 24 h of hydration, as supported by measured values of 0.0148 W/mL water, 0.0092 W/mL water, and 0.0066 W/mL water for the maximum heat flow during the first 24 h for the control, F40, and F60 mixtures, respectively. These values are reasonably close to the ratio of 1:0.6:0.4 that might be expected based simply on the cement volume fractions in the three mixtures, if the Class F

**Table 3**  
Setting and hydration apparent activation energies for 15 °C vs. 25 °C results.

Mixture	15 °C Initial setting time (h)	25 °C Initial setting time (h)	Setting $t_{25}/t_{15}$	$E_A$ (setting) (kJ/mol)	Hydration $t_{25}/t_{15}$	$E_A$ (hydration) (kJ/mol)
Control	3.93	2.39	0.608	35.5	0.54	44.0
L10	3.34	2.20	0.659	29.8	0.57	40.2
L10coarse	4.31	2.63	0.610	35.3	0.55	42.7
F40	6.96	3.43	0.493	50.5	0.50	49.5
F30L10	4.21	2.48	0.589	37.8	0.50	49.5
C40	10.56	5.09	0.482	52.1	0.52	46.7
C30L10	6.95	3.86	0.555	42.0	0.52	46.7
F60	7.92	5.12	0.646	31.2	0.515	47.4
F45L15	4.74	3.28	0.692	26.3	0.53	45.4
C60	16.01	9.01	0.563	41.1	0.555	42.1
C45L15	8.15	4.85	0.595	37.1	0.535	44.7
Average				38.1		45.3
Std. Dev.				8.0		3.0

**Table 4**  
Setting and hydration apparent activation energies for 25 °C vs. 40 °C results.

Mixture	25 °C Initial setting time (h)	40 °C Initial setting time (h)	Setting $t_{40}/t_{25}$	$E_A$ (setting) (kJ/mol)	Hydration $t_{40}/t_{25}$	$E_A$ (hydration) (kJ/mol)
Control	2.39	1.69	0.707	17.9	0.513	34.5
L10	2.20	1.45	0.659	21.6	0.476	38.4
L10coarse	2.63	1.71	0.650	22.3	0.526	33.2
F40	3.43	1.97	0.574	28.7	0.513	34.5
F30L10	2.48	1.61	0.649	22.4	0.513	34.5
C40	5.09	3.53	0.694	18.9	0.513	34.5
C30L10	3.86	2.28	0.591	27.2	0.513	34.5
F60	5.12	2.86	0.559	30.1	0.526	33.2
F45L15	3.28	1.75	0.534	32.5	0.513	34.5
C60	9.01	4.55	0.505	35.4	0.476	38.4
C45L15	4.85	2.77	0.571	29.0	0.488	37.1
Average				26.0		35.2
Std. Dev.				5.7		1.9

fly ash were indeed totally inert. In summary, based on the calorimetry measurements conducted at 15 °C and 25 °C, the Class F fly ash is relatively inert during the first 24 h of hydration, the fine CaCO<sub>3</sub> accelerates and amplifies the early-age hydration but doesn't alter its temperature sensitivity, and the Class C fly ash, while initially retarding the hydration, is quite reactive at early ages, with an apparent activation energy that is likely different from that of the ordinary Portland cement (OPC).

As the hydration temperature is raised from 25 °C to 40 °C, all of the mixtures in Fig. 4 indicate that a single apparent activation energy is no longer capable of describing the complete composite set of hydration/pozzolanic reactions. While in each case, the 40 °C heat flow results have been successfully time-transformed to match the initial rise corresponding to the primary silicate peak obtained at 25 °C, the subsequent aluminate reactions no longer overlap each other for any of the 11 mixtures. The higher and earlier time-transformed data for these aluminate reactions at 40 °C would once again indicate a higher apparent activation energy than that found for the silicate reactions, as observed for the 15–25 °C data sets for the Class C fly ash mixtures. It is well known that the content and form of calcium sulfate (and any other sulfates present in the cement clinker and fly ash) has a large influence on these reactions [27,28], and the variable solubility (and stability) of these sulfate phases as a function of temperature could certainly be one contributor to the observed differences in apparent activation energy.

In examining the values in Tables 3 and 4, it is quite clear that the apparent activation energies for setting are different from those for hydration for these ternary blends. Furthermore, while the apparent activation energies determined for hydration for the 11 different mixtures could arguably be characterized by a single average value, with coefficients of variation of only 6.6% and 5.4%

in Tables 3 and 4, respectively, those for setting exhibit a much greater dispersion with coefficients of variation of about 21% in both cases. Previously, Ezziane et al. [12] found activation energies on the order of 18 kJ/mol for OPC and limestone-blended cements when evaluating initial setting time at temperatures from 20 °C to 60 °C, in reasonable agreement with the values of 18 kJ/mol and 22 kJ/mol determined for the control and L10 mixtures, respectively, in going from 25 °C to 40 °C in Table 4. In their study, slightly higher values were determined for mixtures incorporating either a natural pozzolan or slag. Lei and Struble [26] determined an apparent activation energy of about 22 kJ/mol for an OPC system, based on measuring early age yield stress vs. temperature from 25 °C to 65 °C. For a variety of OPC mixtures and mixtures with either fly ash or slag and with curing temperatures varying within a limited range for cold, control, and hot conditions, Wade et al. [16] determined activation energy values ranging from 23.3 kJ/mol to 35.2 kJ/mol for setting. In contrast, for OPC mixtures, Pinto and Hover [14] found an apparent activation energy of 40.9 kJ/mol for the time until initial set for mortar temperatures between 10 °C and 35 °C, although the initial mixing temperature was not matched to the curing temperature in their study, with all mixtures being initially prepared at a temperature of about 30 °C. In general, these previous values are in reasonable agreement with the range of values determined in the current study. While the average apparent activation energy for hydration from 25 °C to 40 °C (35.2 kJ/mol) is about 10 kJ/mol less than that for hydration from 15 °C to 25 °C (45.3 kJ/mol), their overall average value is in good agreement with the default value of 40 kJ/mol recommended for strength prediction in the ASTM C1074 standard test method [19]. Furthermore, the trends observed in the present study are quite consistent with the field results of Nixon et al. [29], who determined activation energies

of 33.5 kJ/mol and 40.0 kJ/mol for warm-weather and cold-weather concrete placements, respectively.

As shown in Fig. 5, for most of the mixtures and conditions examined in this study, the apparent activation energy for setting was less than that determined for hydration from the isothermal calorimetry curves. Hydration and setting are clearly related processes, as the latter requires the former. However, while hydration is primarily a chemical process, setting is a physical consequence of the volume and location of hydration products that are formed by the ongoing chemical reactions [26,30–32]. One would expect that for the current mixtures without any admixtures, the cement particles would be highly flocculated, thereby providing a backbone structure upon which the precipitation and growth of hydration products would induce setting. It is quite likely that the degree of flocculation and the geometric/topological characteristics of this backbone structure are dependent upon both temperature and the mixing energy that are imparted to each mixture. For example, as the (mixing) temperature is varied from 15 °C to 40 °C, the viscosity of water decreases by a factor of 1.75 [33], which should surely have an influence on the dispersion during mixing and subsequent (re)flocculation of the cement particles in each mixture. A lower value for the apparent activation energy for setting vs. that for hydration would imply that less hydration is required to achieve setting as temperature is decreased, perhaps due to either a more strongly flocculated arrangement of particles or a more localized formation of (perhaps stiffer) hydration products within the more viscous pore solution.

It should be noted from Table 3 that in every case, the incorporation of fine CaCO<sub>3</sub> into a binary blend with cement or a ternary blend with cement and fly ash (Class C or Class F) further lowers the apparent activation energy for setting (relative to the counterpart mixture without CaCO<sub>3</sub>) and thus should reduce the cold weather sensitivity of these mixtures. Understandably, this is a desirable outcome, as the delay in initial setting time due to reduced hydration rates at lower temperatures is at least partially offset by the replacement of a portion of the cement with fine CaCO<sub>3</sub> powder. In contrast, the coarser CaCO<sub>3</sub> powder did not significantly change the apparent activation energy for setting when incorporated into the OPC mixture. From Table 3, the influence of the fine CaCO<sub>3</sub> is more dramatic for the mixtures with a 40% cement replacement than for those with a 60% replacement, but it is significant in both cases.

In progressing from OPC mixtures through binary blends with fine CaCO<sub>3</sub> or fly ash to ternary mixtures with all three powders, it is of interest to consider which particles are flocculating and contributing to the solid skeleton that is critical to setting and subsequent early-age strength development. For a fairly inert Class F fly ash, such as the one used in this study, past investigations have indicated that the fly ash particles do not likely participate in the

flocculation and setting processes, as the measured yield stress was found to be only a function of the cement particle density within the three-dimensional microstructure [34]. In this case, the fly ash functions mainly as a diluent at early ages, lowering the system's yield stress and increasing its setting times. On the other hand, the Class C fly ash used in this study is hydraulic in its own right and will flash set when mixed directly with water. Thus, the Class C fly ash particles could contribute to the setting process by flocculating with the cement particles and/or serving as precipitation and reaction sites that assist in linking up a three-dimensional percolated solid backbone. Unfortunately, this Class C fly ash substantially retards cement hydration (Fig. 4) so that any of its potentially beneficial reactions are more than offset by the delays it produces in the binary (and to a lesser extent in the ternary) blends.

This leaves only consideration of the fine CaCO<sub>3</sub> powder and its fate in the setting process. Valuable information has been provided in the studies of Sato et al. [35,36], along with the earlier research of Ramachandran and Zhang [37]. These authors noted two key items based on scanning electron microscopy observations and concurrent calorimetry measurements. First, the small (down to nano size in their study) CaCO<sub>3</sub> particles have a definite tendency to stick to the larger cement particles. Second, hydration products appear to be equally comfortable precipitating and growing on CaCO<sub>3</sub> as on cement clinker surfaces. This evidence would suggest that the fine CaCO<sub>3</sub> particles will be active participants in creating a percolated three-dimensional network of solids (i.e., initial setting). It must also be recognized that having fine CaCO<sub>3</sub> particles participate in the setting process could be quite different from having similarly-sized fine cement particles do so, due to their large differences in reactivity. While many fine cement particles of 1 μm diameter or less would be expected to completely dissolve at early ages and thus be removed from any developing backbone and perhaps even disconnect some previously formed solid bridges, the less reactive CaCO<sub>3</sub> particles almost certainly do not completely dissolve and therefore should provide a more stable scaffolding for the precipitation and growth of hydration products into a percolated network.

This role of CaCO<sub>3</sub> in setting was further investigated using a three-dimensional cement hydration model (CEMHYD3D, version 3.0) [38]. Previously, the percolation of solids in the hydration model has been shown to correspond closely to needle penetration measurements for OPC pastes prepared at w/c ranging from 0.3 to 0.45 [39]. The measured PSDs for the cement and CaCO<sub>3</sub> powder, along with the estimated Bogue composition of the cement, were used to create starting three-dimensional microstructures for the control and L10 mixtures in which the cement and CaCO<sub>3</sub> particles were flocculated into a single floc structure. Hydration was executed and a variety of properties including heat release and percolation of solids were monitored. The model's time scale was adjusted to provide a reasonable fit of the model to the experimental heat flow curves (Fig. 6) and the percolation of solids was examined under two scenarios, with and without the CaCO<sub>3</sub> particles being considered as active participants in the three-dimensional burning algorithm employed to assess solids percolation. As can be seen in Fig. 6, while not a perfect fit, the inclusion of the CaCO<sub>3</sub> in the setting computation clearly provides the better fit to the experimental data, shifting the percolation curve to earlier times and thus reducing the initial setting time.

The results in Fig. 6 indicate that CaCO<sub>3</sub> could accelerate the setting process but do not directly address the reduced apparent activation energy for the L10 relative to the control OPC mixture. There are several potential contributors to less hydration being required to achieve setting in the L10 mixture as temperature is lowered. The modification of the flocculated structure that provides the backbone for the setting skeleton has been mentioned previously.

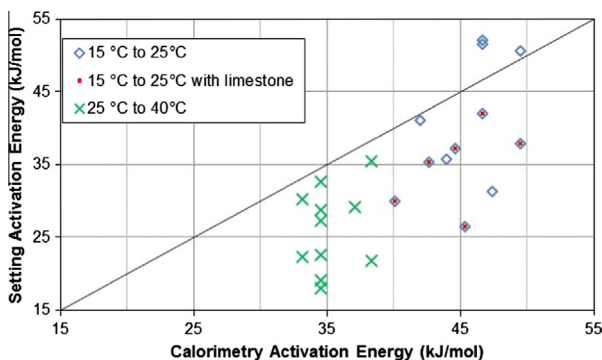


Fig. 5. Comparison of apparent activation energies determined for hydration and initial setting for the various mixtures.

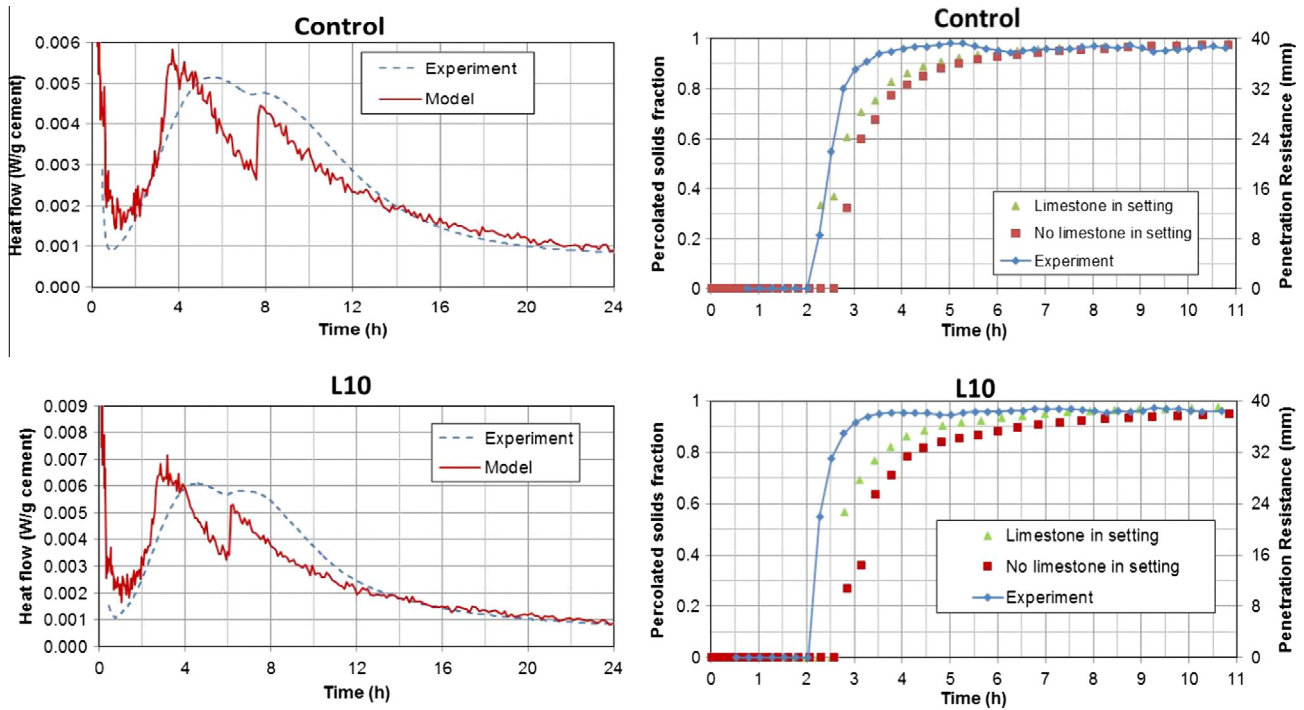


Fig. 6. CEMHYD3D model predictions and experimental results for heat flow (left) and setting (right) for control and L10 mixtures.

Another contribution could be provided due to the fact that the solubility of  $\text{CaCO}_3$ , unlike that of most minerals, actually increases as temperature is reduced [40,41]. Thus, the  $\text{CaCO}_3$  powder should be more soluble at 15 °C than at 25 °C. The stiffer carboaluminate phases that would be formed as the  $\text{CaCO}_3$  reacts in the binary and ternary blends could then contribute to an increased penetration resistance. Additionally, precipitation and growth of hydration products on the fine  $\text{CaCO}_3$  particles that are bridging larger particles in the three-dimensional microstructure could be enhanced at lower temperatures. Further research is required to determine the reality and magnitude of these hypothesized contributing factors to the reduced apparent activation energy for setting at low temperatures in the presence of  $\text{CaCO}_3$ .

The reactivity of the  $\text{CaCO}_3$  in the binary and ternary blends was further examined based on thermogravimetric analysis. Table 5 contains the results obtained for estimated calcium hydroxide and calcium carbonate contents of the five raw materials employed in this study, while the subsequent results at ages of 1 d and 7 d for  $\text{Ca(OH)}_2$  and  $\text{CaCO}_3$  for hydrated systems are provided in Tables 6 and 7, respectively. In Tables 6 and 7, two determinations (separate mixtures) are shown for the F60 mixture at 15 °C to provide some indication of measurement uncertainty. In Table 5, the estimated  $\text{CaCO}_3$  content, equivalent to 3.68% on a per g initial material basis, compares quite favorably with the value of 3.66% reported by the

cement manufacturer and the estimated  $\text{CaCO}_3$  contents of the two  $\text{CaCO}_3$  powders indicate that they are indeed of a high purity (>95%).

The calcium hydroxide contents in Table 6 indicate the expected acceleration of hydration with increasing temperature and the accelerating influence of the fine  $\text{CaCO}_3$  at 1 d in its binary blend with cement (L10 mixture). In general, the Class F fly ash reduces the  $\text{Ca(OH)}_2$  content at these early ages, but mainly due to a diluent effect as opposed to a substantial pozzolanic reaction. The Class C fly ash is reactive at early ages, but its influence on  $\text{Ca(OH)}_2$  content is complicated in that this fly ash contains a substantial CaO content and can thus be both a source of and a sink for  $\text{Ca(OH)}_2$ . For the ternary blends at 1 d, in every case, the replacement of fly ash with the fine  $\text{CaCO}_3$  powder increases the estimated  $\text{Ca(OH)}_2$  content, consistent with its acceleration of the early age hydration reactions (Fig. 4). This effect is not as dramatic at 7 d, as the increase in  $\text{Ca(OH)}_2$  content due to increased cement hydration can be partially offset by increased consumption of  $\text{Ca(OH)}_2$  in its pozzolanic reactions with the fly ash and/or its participation in the formation of carboaluminates with the fine  $\text{CaCO}_3$  powder.

Table 5  
Estimated  $\text{Ca(OH)}_2$  and  $\text{CaCO}_3$  contents for the raw materials (on a per g ignited material basis).

Powder	$\text{Ca(OH)}_2$ (%)	$\text{CaCO}_3$ (%)
Cement	0.73	3.47
C ash	0.20	0.10
F ash	0.57	0.24
Fine $\text{CaCO}_3$	2.28	178.2 <sup>a</sup>
Coarse $\text{CaCO}_3$	0.29	171.1

<sup>a</sup> Pure  $\text{CaCO}_3$  would have a value of (molar mass of  $\text{CaCO}_3$ /molar mass of  $\text{CaO}$ ) = 100.09/56.08 = 178.5%.

Table 6  
Estimated  $\text{Ca(OH)}_2$  contents for the mixtures.

Mixture	Initial (%)	1 d (15 °C, 25 °C, 40 °C)			7 d (15 °C, 25 °C, 40 °C)		
Control	0.73	14.6%	14.9%	22.0%	24.0%	26.0%	26.3%
L10	0.81	15.9%	18.6%	23.1%	24.2%	25.3%	27.2%
L10coarse	0.70	14.3%	17.6%	19.9%	23.1%	24.9%	26.2%
F40	0.68	9.5%	14.0%	16.5%	17.8%	19.2%	19.8%
F30L10	0.78	10.8%	14.8%	17.8%	18.8%	15.9%	20.8%
C40	0.53	8.2%	11.3%	14.9%	16.5%	24.8%	19.6%
C30L10	0.66	10.4%	13.3%	15.5%	17.7%	18.7%	20.8%
F60	0.63	7.8%	10.9%	12.4%	14.2%	N.M. <sup>a</sup>	13.5%
				7.5%			14.2%
F45L15	0.89	8.4%	11.5%	13.9%	14.9%	15.9%	14.9%
C60	0.42	3.8%	6.8%	9.5%	11.5%	13.0%	14.5%
C45L15	0.68	6.0%	N.M.	11.0%	12.3%	14.0%	14.2%

<sup>a</sup> N.M. = not measured.

**Table 7**  
Estimated CaCO<sub>3</sub> contents for the mixtures.

Mixture	Initial (%)	1 d (15 °C, 25 °C, 40 °C)			7 d (15 °C, 25 °C, 40 °C)		
Control	3.5	3.9%	3.3%	3.9%	3.8%	3.9%	3.8%
L10	12.5	12.2%	12.0%	11.9%	11.5%	11.6%	11.7%
L10coarse	12.3	12.6%	12.8%	12.7%	12.3%	12.5%	12.4%
F40	2.4	2.8%	2.8%	2.8%	2.7%	3.0%	2.8%
F30L10	12.6	11.9%	12.1%	12.0%	11.6%	11.5%	11.8%
C40	2.2	2.5%	2.5%	2.6%	2.5%	3.7%	2.7%
C30L10	12.0	11.5%	11.0%	11.1%	11.0%	10.6%	10.8%
F60	1.8	2.1%	2.1%	2.3%	2.1%	N.M. <sup>a</sup>	2.2%
		2.1%			2.2%		
F45L15	18.5	N.M.	17.7%	17.1%	16.0%	17.7%	17.1%
C60	1.6	2.2%	2.1%	1.9%	2.0%	2.0%	2.5%
C45L15	17.0	16.1%	N.M.	15.1%	15.5%	13.5%	14.8%

<sup>a</sup> N.M. = not measured.

The results in Table 7 indicate the greater reactivity of the fine CaCO<sub>3</sub> vs. its coarser counterpart in the binary blend with OPC. Assuming that the CaCO<sub>3</sub> powder in the cement/fly ash binary blends will be relatively inert, their (increased) CaCO<sub>3</sub> contents relative to their initial values were used to estimate the average extent of carbonation of the specimens at ages of 1 d and 7 d, an increase of about 0.4% in CaCO<sub>3</sub> in most cases. These values were used in turn to adjust the measured values at 1 d and 7 d for the binary (CaCO<sub>3</sub>) and ternary blends in order to calculate an estimated reactivity of the CaCO<sub>3</sub> powder in these blends, with the obtained estimates being provided in Table 8. Once again, the enhanced reactivity of the finer CaCO<sub>3</sub> is seen in comparing the L10 and L10coarse mixtures' results in Table 8. The reactivity of the coarse CaCO<sub>3</sub> at 1 d is negligible and it continues to be significantly less than that of the fine CaCO<sub>3</sub> at 7 d, consistent with its reduced acceleration of cement hydration, as illustrated by the 40 °C isothermal calorimetry results compared in Fig. 4. The estimated reactivity of the fine CaCO<sub>3</sub> is further enhanced in the ternary blends with fly ash, as this combination of powders exhibits a synergy with respect to hydration and strength [4,10].

While strength was not measured in this current study on pastes, some expectations can be inferred based on the cumulative heat release values measured for the different mixtures [23]. For example, for predicting relative 7 d strengths, the 7 d cumulative heat release values (per mL initial water) for the 11 mixtures are plotted vs. temperature in Fig. 7. The results suggest that for two of the three curing temperatures, the L10 mixture should offer comparable 7 d strengths to the control mixture and that the mixtures with Class C fly ash will offer superior strengths in comparison to those with Class F fly ash; the latter has indeed been observed in actual concrete mixtures prepared at about 25 °C [9,10]. The replacement of fly ash by fine CaCO<sub>3</sub> powder should also increase 7 d strengths for the 25 °C mixtures, and even more so for the 15 °C mixtures. Once again at 25 °C, actual mixtures have indicated significantly higher strengths at 7 d (and beyond) in those ternary blend concretes with CaCO<sub>3</sub> replacement for fly ash [9,10].

**Table 8**  
Estimated reaction (% remaining) of CaCO<sub>3</sub> in the mixtures.

Mixture	1 d (15 °C, 25 °C, 40 °C)			7 d (15 °C, 25 °C, 40 °C)		
L10	94.7%	93.4%	92.2%	89.8%	90.5%	89.3%
L10coarse	99.0%	100.9%	99.8%	97.0%	98.7%	96.1%
Mixtures with Class C or Class F fly ash (40L10 and 45L15)	15 °C = 92.1% ± 0.8% <sup>a</sup>			15 °C = 88.0% ± 2.2%		
	25 °C = 91.7% ± 2.7%			25 °C = 86.0% ± 6.7%		
	40 °C = 89.5% ± 2.0%			40 °C = 88.3% ± 2.7%		

<sup>a</sup> ± Value indicates standard deviation from three or four mixtures at each temperature and age.

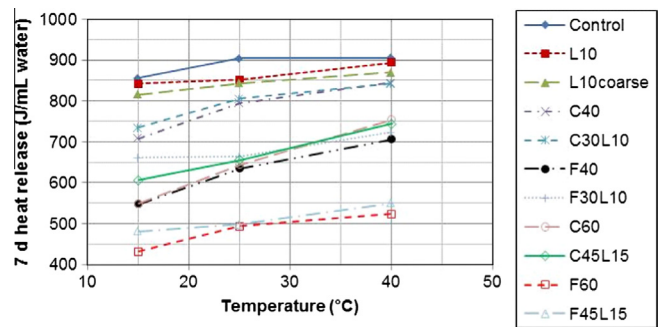


**Fig. 7.** 7 d cumulative heat release vs. curing temperature for the 11 different paste mixtures.

#### 4. Conclusions

Apparent activation energies for setting and hydration have been determined for a variety of binary and ternary blends of cement, CaCO<sub>3</sub> powder, and fly ash, prepared at a constant water volume fraction. Based on the results presented here, the following conclusions can be drawn.

- (1) For hydration, the applicability or lack thereof of a single apparent activation energy to describe the complete early-age hydration process can best be assessed based on time transformations of the heat flow isothermal calorimetry curves.
- (2) Apparent activation energies for setting and hydration can be different, as the first depends on the development of a physical skeleton (backbone) of flocculated cement/CaCO<sub>3</sub> particles and hydration products, and the latter is chiefly a chemical process.
- (3) For the mixtures investigated in this study, the apparent activation energy for hydration could be adequately described by a single (average) value with a coefficient of variation on the order of 6% for both the 15–25 °C and the 25–40 °C data sets. However, the apparent activation energy for hydration is less for the higher temperature range than for the lower one.
- (4) For setting, there is a greater dispersion in the values of apparent activation energy, but one clear trend is that the replacement of either cement or fly ash by fine CaCO<sub>3</sub> reduces the apparent activation energy for the lower temperature conditions. This highlights another potential benefit of the fine CaCO<sub>3</sub> in ternary blends, namely reducing the low temperature sensitivity of high volume fly ash concrete mixtures.
- (5) The reactivity of the CaCO<sub>3</sub>, as well as its ability to accelerate and amplify the cement hydration reactions, is influenced greatly by its particle size (surface area), with the 1 μm CaCO<sub>3</sub> powder being far superior to the 17 μm CaCO<sub>3</sub> in this study.
- (6) For the fine CaCO<sub>3</sub> mixed with OPC, about 10% of the initial CaCO<sub>3</sub> powder has been consumed (reacted) by an age of 7 d. In the ternary blends, this consumption is increased further by a few percent.

#### Acknowledgements

The author would like to thank Amzaray Ahmed, Luis Manrique, and Max Peltz for their assistance with the experimental measurements at NIST. The provision of materials by Lafarge, the Lehigh Cement Company, OMYA, Inc., and Separation Technologies, LLC is gratefully acknowledged, as are useful discussions with Dr. Jussara Tanesi of SES Group & Associates, LLC.

## References

- [1] Malhotra VM, Mehta PK. High-performance, high-volume fly ash concrete (for building durable and sustainable structures). 4th ed. Ottawa: Supplementary Cementing Materials for Sustainable Development; 2012.
- [2] Cost VT. Concrete sustainability versus constructability—closing the gap. In: 2011 International concrete sustainability conference, Boston; 2011. <<http://www.nrmcaevents.org/?nav=display&file=189>> [accessed 17.08.13].
- [3] Bentz DP, Ferraris CF, Snyder KA. Best practices guide for high-volume fly ash concretes: assuring properties and performance. NIST technical note 1812. U.S. Department of Commerce; September 2013.
- [4] De Weerd K, Kjellsen KO, Sellevold E, Justnes H. Synergy between fly ash and limestone powder in ternary cements. *Cem Concr Compos* 2010;33(1):30–8.
- [5] Mounanga P, Khokhar MIA, El Hachem R, Loukili A. Improvement of the early-age reactivity of fly ash and blast furnace slag cementitious systems using limestone filler. *Mater Struct* 2011;44:437–53.
- [6] De Weerd K, Ben Haha M, Le Saout G, Kjellsen KO, Justnes H, Lothenbach B. Hydration mechanisms of ternary Portland cements containing limestone powder and fly ash. *Cem Concr Res* 2011;41:279–91.
- [7] Bentz DP, Sato T, de la Varga I, Weiss WJ. Fine limestone additions to regulate setting in high volume fly ash mixtures. *Cem Concr Compos* 2012;34(1):11–7.
- [8] Gurney L, Bentz DP, Sato T, Weiss WJ. Reducing set retardation in high volume fly ash mixtures with the use of limestone: improving constructability for sustainability. *Transp Res Rec J Transp Res Board Concr Mater* 2012:139–46.
- [9] Tanesi J, Bentz DP, Ardani A. Enhancing high volume fly ash concretes using fine limestone powder. In: ACI SP-294: advances in green binder systems. Farmington Hills, MI: American Concrete Institute; 2013.
- [10] Bentz DP, Tanesi J, Ardani A. Ternary blends for controlling cost and carbon content. *Concr Int* 2013;35(8):51–9.
- [11] Moon J, Oh JE, Balonis M, Glasser FP, Clark SM, Monteiro PJM. High pressure study of low compressibility tetracalcium aluminum carbonate hydrates  $3\text{CaO}\cdot\text{Al}_2\text{O}_3\cdot\text{CaCO}_3\cdot 11\text{H}_2\text{O}$ . *Cem Concr Res* 2012;42:105–10.
- [12] Ezziane K, Kadri EH, Hallal A, Duval R. Effect of mineral additives on the setting of blended cement by the maturity method. *Mater Struct* 2010;43(3):393–401.
- [13] De Weerd K, Ben Haha M, Le Saout G, Kjellsen KO, Justnes H, Lothenbach B. The effect of temperature on the hydration of composite cements containing limestone powder and fly ash. *Mater Struct* 2012;45:1101–14.
- [14] Pinto RCA, Hover KC. Application of maturity approach to setting times. *ACI Mater J* 1999;96(6):686–91.
- [15] Schindler AK. Prediction of concrete setting. In: Weiss J, Kovler K, Marchand J, Mindess S, editors. Proceedings of the RILEM international symposium on advances in concrete through science and engineering. Illinois: RILEM Publications SARL; 2004.
- [16] Wade SA, Nixon JM, Schindler AK, Barnes RW. Effect of temperature on the setting behavior of concrete. *J Mater Civ Eng* 2010;22(3):214–22.
- [17] Pang X, Bentz DP, Meyer C, Funkhouser GP, Darbe R. A comparison study of Portland cement hydration kinetics as measured by chemical shrinkage and isothermal calorimetry. *Cem Concr Compos* 2013;39:23–32.
- [18] Carino NJ. The maturity method: theory and applications. *Cem Concr Aggr* 1984;6(2):61–73.
- [19] ASTM International. ASTM C1074-11 Standard practice for estimating concrete strength by the maturity method. West Conshohocken, PA: ASTM International; 2011. 10 pp.
- [20] Vance K, Aguayo M, Oey T, Sant G, Neithalath N. Hydration and strength development in ternary Portland cement blends containing limestone and fly ash or metakaolin. *Cem Concr Compos* 2013;39:93–103.
- [21] ASTM International. ASTM C191-08 Standard test methods for time of setting of hydraulic cement by Vicat needle. West Conshohocken, PA: ASTM International; 2008. 8 pp.
- [22] ASTM International. ASTM C403/C403M-08 Standard test methods for time of setting of concrete mixtures by penetration resistance. West Conshohocken, PA: ASTM International; 2008. 7 pp.
- [23] Bentz DP, Barrett T, De la Varga I, Weiss WJ. Relating compressive strength to heat release in mortars. *Adv Civ Eng Mater* 2012;1(1): 14 pp.
- [24] Kumar A, Oey T, Kim S, Thomas S, Badran S, Li J, et al. Simple methods to estimate the influence of limestone fillers on reaction and property evolution in cementitious materials. *Cem Concr Compos* 2013;42:20–9.
- [25] Taylor HF. *Cement chemistry*. 2nd ed. London: Thomas Telford; 1997.
- [26] Lei W-G, Struble L. Microstructure and flow behavior of fresh cement paste. *J Am Ceram Soc* 1997;80(8):2021–8.
- [27] Lerch W. The influence of gypsum on the hydration and properties of Portland cement pastes. *PCA Bulletin* 12. Chicago, IL: Research Laboratory of the Portland Cement Association; March 1946.
- [28] Niemuth MD, Barcelo L, Weiss J. Effect of fly ash on optimum sulfate levels measured using heat and strength at early ages. *Adv Civ Eng Mater* 2012;1(1):18 pp.
- [29] Nixon JM, Schindler AK, Barnes RW, Wade SA. Evaluation of the maturity method to estimate concrete strength in field applications. Research report no. 2. Alabama Department of Transportation, ALDOT Research Project 930-950; February 2008.
- [30] Jiang SP, Mutin JC, Nonat A. Analysis of the hydration-setting relation: towards a comprehensive approach of the cement setting. In: Proceedings of the 9th international congress on the chemistry of cement, vol. IV, New Delhi; 1992. p. 17–23.
- [31] Sant G, Ferraris CF, Weiss J. Rheological properties of cement pastes: a discussion of structure formation and mechanical property development. *Cem Concr Res* 2008;38:1286–96.
- [32] Sant G, Dehadrai M, Bentz D, Lura P, Ferraris CF, Bullard JW, et al. Detecting the fluid-to-solid transition in cement pastes. *Concr Int* 2009;31(6):53–8.
- [33] Kestin J, Sokolov M, Wakeham WA. Viscosity of liquid water in the range  $-8\text{ }^{\circ}\text{C}$  to  $150\text{ }^{\circ}\text{C}$ . *J Phys Chem Ref Data* 1978;7(3):941–8.
- [34] Bentz DP, Ferraris CF, Galler MA, Hansen AS, Guynn JM. Influence of particle size distribution on yield stress and viscosity of cement–fly ash pastes. *Cem Concr Res* 2012;42(2):404–9.
- [35] Sato T, Diallo F. Seeding effect of nano- $\text{CaCO}_3$  on the hydration of tricalcium silicate. *Transp Res Record J Transp Res Board* 2010;2141:61–7.
- [36] Sato T, Beaudoin J. Effect of nano- $\text{CaCO}_3$  on hydration of cement containing supplementary cementitious materials. *Adv Cem Res* 2011;23(1):1–11.
- [37] Ramachandran VS, Zhang C. Influence of  $\text{CaCO}_3$  on hydration and microstructural characteristics of tricalcium silicate. *II Cemento* 1986;83:129–52.
- [38] Bentz DP. Modeling the influence of limestone filler on cement hydration using CEMHYD3D. *Cem Concr Compos* 2006;28(2):124–9.
- [39] Bentz DP. Cement hydration: building bridges and dams at the microstructure level. *Mater Struct* 2007;40(4):397–404.
- [40] Weyl PK. The change in solubility of calcium carbonate with temperature and carbon dioxide content. *Geochim Cosmochim Acta* 1959;17(3–4):214–25.
- [41] Brecevic L, Nielsen AE. Solubility of amorphous calcium carbonate. *J Cryst Growth* 1989;98:504–10.